Synthesis of multi-walled carbon nanotubes by thermal CVD technique on NiO catalyst

Raad Q. Abdalamir[1], a, Ziad T. Khodair[2*], Ahmed N. Abd[3]
[1]Department of Physics, College of Science, University of Diyala, Diyala, Iraq.
[2]Department of Chemistry, College of Science, University of Diyala, Iraq.
Corresponding author
Email: ziad_tariq70@yahoo.com

Abstract
In our work, carbon nanotubes (CNTs) were grown by using NiO as a catalyst, using chemical vapor deposition (CVD). and using propanol (C3H8O) as a carbon source, under specific conditions such as reaction temperature, time, and gas ratio that are 740 C, 30 min, and 125 Sccm, respectively. Specifications of CNTs were analyzed and characterized using X-ray diffraction (XRD), the field emission scanning electron microscope (FESEM) with energy-dispersive X-ray spectroscopy (EDX), transmission electron microscopic (TEM). showed the results of x-ray diffraction analyzes showed that the sample is the polycrystalline and hexagonal type with a predominant direction (002). Pictures of FE-SEM showed the formation of carbon tubes in various and various forms with NiO aggregates, and the rate obtained at the average sizes of MWCNT was 18.85 nm, As for images of TEM, they demonstrated the formation of multi-walled carbon nanotubes with high clarity. EDS analysis also showed Primarily carbon and then nickel and have discernible peaks in the figure, with a few molybdenum and cobalt impurities showing up. As for images TEM, they demonstrated the formation of multi-walled carbon nanotubes with high clarity.
Keywords: synthesis; carbon nanotubes; characterization; chemical vapor deposition; NiO as a catalyst

1. Introduction

Although carbon nanotubes are difficult to create and expensive, the new carbon material consists of carbon nanotubes (CNTs), which appear to have become a reality for the world thanks to Iijima, who prepared one type of single-walled carbon nanotube in 1991 with Ichihashi [1]. Because the tubes are filtered during the manufacturing process to remove impurities, they have a lot of potentials and uses in the present and future, including electrical, optical, and thermal conductivity, tensile strength, and chemical reaction. They are also employed in sensors [2] and lithium batteries [3] due to their exceptional flexibility. As a result, several attempts to prepare it appeared, resulting in a progressive drop in the cost of manufacturing and purifying. Chemical Vapor Deposition (CVD) [4] and Arc-Discharge [5] are two primary methods for the manufacture of carbon nanotubes, as are Laser Ablation Technology [6] and Flame Method [7] The CVD method offers the highest chance of obtaining nanotubes with predetermined qualities based on a regulated procedure. [8]. The process involves passing hydrocarbon vapor through a tubular reactor with a precipitation catalyst at a high temperature of 600-1200°C, which is sufficient to break the hydrocarbon bonds in the case of liquid hydrocarbon (gasoline, alcohol, etc.). the liquid is heated in a special compartment and an inert gas is passed through it, which then carries hydrocarbon vapor to the precipitation zone.[9]. The results also demonstrated that the catalyst's effect on carbon nanotubes may be related to the catalyst's nature and the carbon in the catalyst's growth potential. The suggested mechanism for catalytic nanoparticle creation generates a wide range of sizes and geometries, which are influenced by a variety of parameters such as temperature and the chemical composition of the medium. As a result, nickel-based catalysts make it easier to catalyze the formation of multi-walled carbon nanotubes [10]. Regardless of the approach utilized, the temperature is a key factor in controlling the formation of carbon nanotubes. [5].The growth of the MWCNTs was confirmed by field emission scanning electron microscope (FESEM), high-resolution transmission electron microscope (HRTEM), and Raman Spectroscopy.

2. Experimental details

In this study, we used a three-heat zone tube furnace from Nabertherm in the United States. the was a quartz tube with a length of 120 cm and a diameter of 3 cm. The first step in the CVD synthesis of CNTs is the preparation of the catalyst. In our work, we used NiO as a catalyst. and we used a thermal chemical spraying method to deposit NiO films on quartz substrates. The solution is prepared by using Nickel chloride hexahydrate ($NiCL_2.6H_2O$), a solid substance in the form of green powder that serves as a source of nickel ions in the spray solution. The components were dissolved in 30ml of distilled water and stirred for 15 minutes in a magnetic stirrer to ensure complete dissolution of the substance in the distilled water, yielding nickel oxide, a homogeneous green solution. At room temperature, the solution was created in a laboratory setting. The spraying procedure was carried out by establishing

doi.org/10.31838/hiv23.02.171 Received: 17.10.22, Revised: 25.11.22, Accepted: 23.12.22.

the necessary conditions and setting the distance between the Nozzle spray device and the base of the electric heater to (27cm). the temperature at which the films were prepared was (400°C) and 1.3 bar was air pressure. And therefore, The quartz substrates are placed in the CVD furnace's core. Involved was the buildup of CNTs in the furnace. the carbon source was propanol and it has a molecular formula C_3H_8O, which has the symbol 1-propanol was heated for 30 minutes at evaporation temperature on a 25 cm^2 surface area of the catalyst. after 200 Sccm of N_2 was injected into the furnace, which was lowered to 125 Sccm when the temperature reached 740°C at a rate of 3.5°C/min. Finally, until the temperature reached room temperature, we lowered the N_2 flow to 50 Sccm. And as a result, after the propanol vapor particles disintegrate and the carbon particles fritter due to the high temperature (740°C), the formed product is deposited on the catalyst, resulting in MWCNT formation.

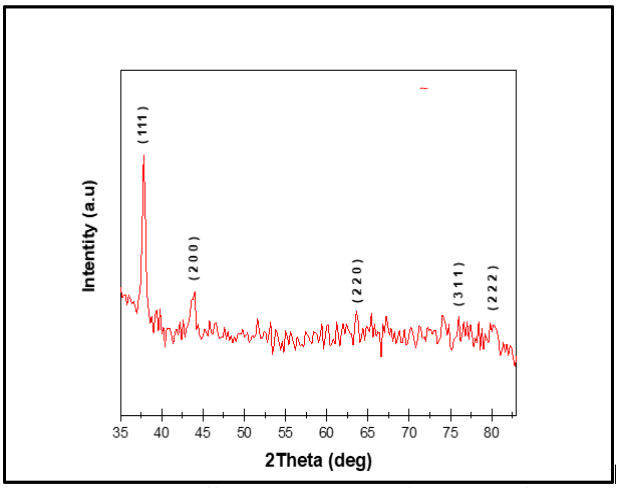

Fig.1. X-ray diffraction pattern of NiO thin film .

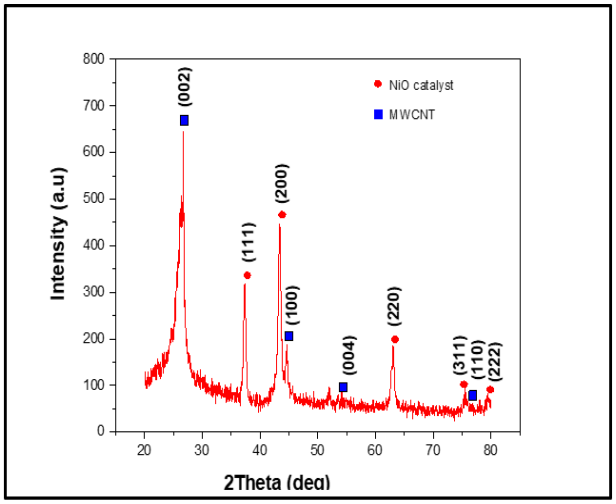

Fig. 2 XRD pattern of NiO/MWCNT

3. Results and Discussions

X-ray diffraction characterization (XRD) and Discussion

Fig. 1 shows the XRD patterns of the prepared NiO thin film showed diffraction peaks at 2θ values of 37.43°, 43.37°, 62.96°, 75.47°, and 79.42° which are attributed to the (111), (200), (220), (311) and (222) crystal planes. The presence of (111), (200), (220), (311), and (222) crystal planes, thus that the NiO films have a polycrystalline structure and have a cubic crystal structure, which matched with the JCPDS card no: 78-0643. , confirms the formation of phase pure NiO.

Fig. 2 shows the XRD patterns of MWCNTs with NiO as a catalyst, it can be noticed that all the samples exhibit diffraction peaks around 2θ ≈ 26.27°, 44.37°, 54.36°, and 76.8° referred to (002),(101),(004), and (110) favorite directions respectively which are in agreement with (IDDC) card number 41-1487. as shown in Table (4.5), The two most important peaks are noted which can be indexed to the reflection (0 0 2) of graphite, and the next peak at 44.34◦ corresponds to the (1 0 0) plane of graphite. The strong peak at 2θ = 26.27° confirmed the crystalline nature of carbon nanotubes with the lattice plane of (0 0 2).

The positions of the peaks and the presence of more than one diffraction peak lead to the conclusion that the samples are polycrystalline in nature with a hexagonal crystalline structure. The presence of nanotubes indicates the cylindrical structure of graphite embedded to form a nest-like structure which was confirmed by using a scanning electron microscope and transmission electron microscopy. While the other peaks at 37.43°, 43.37°, 62.96°,75.47°, and 79.42° in the XRD patterns are assigned to the (111), (200), (220), (311), and (222) crystallographic plane of NiO catalyst. Thus, we have achieved the identity of the material for MWCNTs and NiO catalysts.

3.2 Crystal lattice constants

For the as-prepared NiO nanoparticles, the crystal lattice constants (ao = bo = co) were determined using the Cubic structure relationship, Eq. (1) [11]:

$$\frac{1}{d_{hkl}^2} = \frac{(h^2+k^2+L^2)}{a^2} \quad (1)$$

For MWCNT nanoparticles, the lattice constants (a=b, c) for the hexagonal structure can be calculated by using the formula, Eq. (2) [12] :

$$\frac{1}{d^2} = \frac{4}{3}\left(\frac{h^2+hk+k^2}{a^2}\right) + \frac{\iota^2}{C^2} \quad (2)$$

Where hkl are Miller indices

The plane 111 were used to calculate the lattice constants ao. The value of the lattice constants were also determined to be consistent with the value in the international card number. (78-0643) for NiO catalyst, as for MWCVT, Planes 002 and 100 were used to calculate lattice constants ao and co. The values of the retina constants were also discovered to be consistent with the values in the international card number. (41-1487), Table 1 shows the results. Eq. 3 was used to compute the average crystal size (D av) of the as-prepared nanoparticles using the Scherrer method (SM)[13].

$$D_{av} = \frac{K\lambda}{\beta cos\theta_B} \quad (3)$$

Where: D: represents the crystallite size, κ: the shape factor, λ: the radiation wavelength, β: the full width

at half maximum (FWHM), and B represents Bragg's angle. We have noticed that the crystal size of the prepared NiO is equal to 9.90 nm for the planar (111), while the grain size ranged average for the most substantial three peaks (9.90~ 15.14) nm, and the crystal size of the prepared MWCNT is equal to 5.45 nm for the planar (002). The grain size ranged average for the strongest three peaks (5.45~ 8.94) nm. as shown in Table 1.

Table 1 Structural parameters of the NiO catalyst and MWCNT.

Sample	Values for NiO catalyst	Values for MWCNT
h k l	(111)	(002)
2θ (°)	37.435	26.277
d hkl (Å)	2.400	3.358
FWHM(deg)	0.8472	1.4967
The lattice constants (Å)	ao= 4.157	ao= 2.470, co= 6.777
Dav (nm)	9.90	5.45
δ (nm −2)	0.01020	0.00425
Micro Strain (S)	0.0046688	0.0078371

3.3 Dislocation Density(δ)

Represents the number of dislocation lines that cut a unit area. It can be calculated by the following Eq. (4) [14,15]:

$$\boldsymbol{\delta} = \frac{1}{D_{av}^2} \quad (4)$$

Crystal distortions, or deviation in the lattice constants from their value in the international card, are also known as microstrain (S). We used the lattice constant (C_o) as an example, and microstrain can be calculated using equation (5) [16] :

$$\boldsymbol{S} = [\,|\,C(ASTM) - C(XRD)\,|\,/C(ASTM)\,] \times 100\% \quad (5)$$

3.4 EDS for MWCNT with NiO catalyst

The Energy Dispersive Spectroscopy (EDS) of the produced MWCNT powder with NiO catalyst using the CVD technique is shown in Figure 2a. Primarily carbon and then nickel have discernible peaks in the figure, with a few molybdenum and cobalt impurities showing up. This is related to the powder preparation process prior to the FESEM investigation and the manner of preparation after granulating the nanopowders.

3.4. 1- Scanning Electron Microscopy (FESEM) Results

IN Fig.3a, The morphology and microstructure of the composites prepared from MWCNT/NiO were visualized by SEM with a magnifying power of 100 nm. it can be roughly illustrated that MWCNT were uniformly distributed and microscopically compact by good dispersion of particles with NiO aggregates. The SEM images revealed the presence of irregular shapes and sizes of NiO particles. in Fig.3b,c the average size of catalyst particles for composites was 35.20 nm and The average sizes of MWCNT were 18.85 nm which was slightly larger than XRD measurements. Such difference was probably because of some aggregation interface between NiO catalyst and CNT, which is advantageous for restraining the recombination of photogenerated electron-hole pairs.

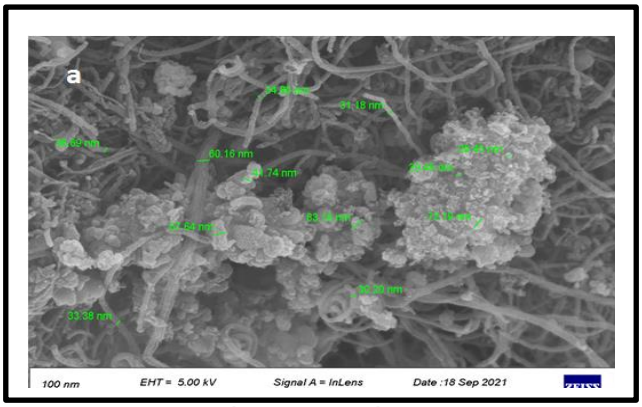

Fig. 3.a. FESEM, of the sample for MWCNT 100.00 kx

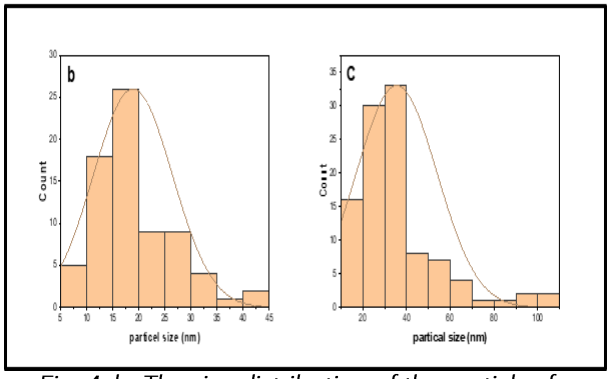

Fig. 4. b. The size distribution of the particles for MWCNT. C. The size distribution of the particles for NiO catalyst.

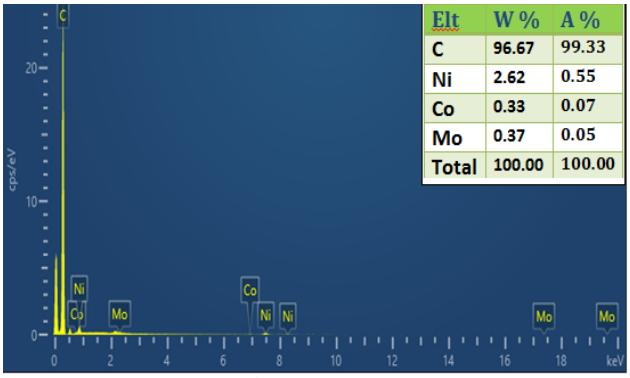

Fig.5 EDS of the prepared MWCNT

3.6 TEM Analysis of the MWCNT Results

The MWCNT nanoparticles prepared by CVD were studied under the TEM. and were used for further investigation of the morphology of CNT/NiO nanocomposites. The TEM images of nanocomposites are shown in Fig. 5.a, b The particle size of NiO obtained is small and uniform according to Fig. 5(a). The diameters of the samples were only about 6 to 15 nm, which was consistent with that of the XRD results. From Fig. 5(a,b), the surface of CNT was clean. The diameters of CNT are about 10 to 16 nm. The surface of the nanotubes is covered with some impurities of NiO particles, which will be due to the possible presence of CNT and NiO peaks and their variance with an increase and decrease in the XRD patterns. The size and shape of the nanoparticles correspond to their size and shape in the FESEM results, and the prepared particles are nanoscale.

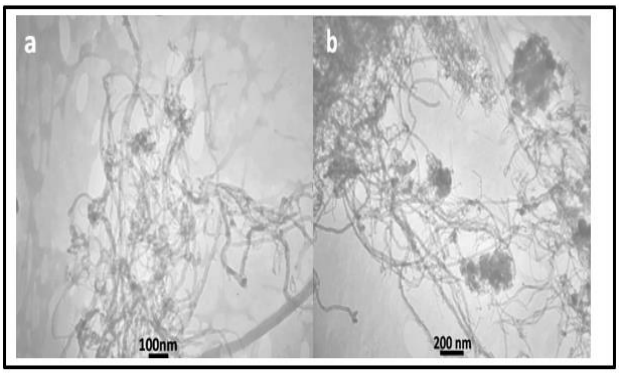

Fig. 6. TEM picture of a: MWCNT 100 nm b: MWCCNT 200 nm.

4. Conclusions

This study reports the growth of MWCNTs on NiO catalyst at 740°C using the CVD technique. The as-prepared catalyst comprises nickel oxide, according to the XRD peak position analysis. based on a FESEM analysis The shape of the particles within the agglomerates is generally spherical, as shown in the TEM images, and it is located within the nanoscale. The growth of MWCNTs was confirmed by FESEM, HRTEM, and Raman Analysis, With the presence of some contaminants and catalyst particles that appeared in the EDS, the FESEM pictures reveal the formation of a network of CNTs. The MWCNT formation was clearly visible in the HRTEM photos. The sample has a low concentration of flaws, according to Raman's analysis.

5. Acknowledgement

The authors express their sincere thanks and gratitude to the Department of physics, College of Science, University of Diyala, Iraq for providing the facilities for all laboratory tests.

References

[1] Iijima, S., & Ichihashi, T. (1993). Single-shell carbon nanotubes of 1-nm diameter. nature, 363(6430), 603-605.
[2] Kong, J., Franklin, N. R., Zhou, C., Chapline, M. G., Peng, S., Cho, K., & Dai, H. (2000). Nanotube molecular wires as chemical sensors. science, 287(5453), 622-625.
[3] Fang, S., Shen, L., Zheng, H., & Zhang, X. (2015). Ge–graphene–carbon nanotube composite anode for high performance lithium-ion batteries. Journal of Materials Chemistry A, 3(4), 1498-1503.
[4] Ferreira, F. V., Franceschi, W., Menezes, B. R., Biagioni, A. F., Coutinho, A. R., & Cividanes, L. S. (2019). Synthesis, characterization, and applications of carbon nanotubes. In Carbon-Based Nanofillers and Their Rubber Nanocomposites (pp. 1-45). Elsevier.
[5] Rahman, G., Najaf, Z., Mehmood, A., Bilal, S., Mian, S. A., & Ali, G. (2019). An overview of the recent progress in the synthesis and applications of carbon nanotubes. C, 5(1), 3.
[6] D. Mahajan. "Carbon Nanotubes: A Review on Synthesis, Electrical and Mechanical Properties and Applications." Asian Journal of Applied Science and Technology, vol. 1, no. 7, pp. 15-29, 2017.
[7] Chu, H., Han, W., Ren, F., Xiang, L., Wei, Y., & Zhang, C. (2018). Flame synthesis of carbon nanotubes on different substrates in methane diffusion flames. ES Energy & Environment, 2(3), 73-81.
[8] Rafique, M. M. A., & Iqbal, J. (2011). Production of carbon nanotubes by different routes-a review. Journal of encapsulation and adsorption sciences, 1(02), 29.
[9] M. Kumar. "Carbon Nanotube Synthesis and Growth Mechanism, Carbon Nanotubes-Synthesis, Characterization, Applications," InTech, pp.147-170, 2011.
[10] W. Han, P. Wang, Y. Wei, H. Chu, Y. Sun, and W. Cao. Progress in the preparation of carbon nanotubes by flame method. Journal of Process Engineering, vol. 19, no. 1, pp. 3-13, 2019.
[11] J. Hook, H.E. Hall, Manchester Physics Series, John Wiley & Sons, ISBN 978-0-471-92804-1, (2010).
[12] Talegaonkar J. and Patil D. R,"Ammonia Gas Sensing Performance of Polyaniline-SnO2", International Journal of Engineering Research and Technology, Vol. 5, No. 10, 2016.
[13] S.R.Elliott,"Physics of amorphous materials", Wiley, 1990.
[14] Z. T. Khodair, M. A. Al-Jubbori, A. M. Shano , F. I. Sharrad, " Study of Optical and Structural Properties of (NiO)1-x(CuO)x Nanostructures Thin Films", Chemical Data Collections, Vol. 28, pp. 1-7, 2020.
[15] Stephens, D. L., & Alford, W. J. (1964). Dislocation Structures in Single-Crystal Al2O3. Journal of the American Ceramic Society, 47(2), 81-86.
[16] Obata, T., Komeda, K., Nakao, T., Ueba, H., & Tatsuyama, C. (1997). Structural characterization of Si0. 7Ge0. 3 layers grown on Si (001) substrates by molecular beam epitaxy. Journal of applied physics, 81(1), 199-204.